Substrate Mediated Single Atom Isolation: Dispersion of Ni and La on γ-Graphyne

Sunkyung Kim,[a] Pablo Gamallo,[*b] Francesc Viñes,[b] Jin Yong Lee[*a] and Francesc Illas[b]

[a] *Department of Chemistry, Sungkyunkwan University, Suwon 16419, Korea*

[b] *Departament de Ciència de Materials i Química Física & Institut de Química Teòrica i Computacional (IQTCUB), Universitat de Barcelona, c/Martí i Franquès 1, 08028 Barcelona, Spain*

ABSTRACT

It is already known the capability of γ-graphyne, a two-dimensional carbon allotrope, to trigger atomic dispersion of Transition Metals (TMs) opening the path of using γ-graphyne for Single Atom (SA) dispersion with possible applications in different fields. The present study is based on density functional theory calculations using the Perdew-Burke-Ernzerhof exchange-correlation functional, with and without including dispersion terms. The calculations reveal that Lanthanum and Nickel atoms binding to γ-graphyne is stronger than in their corresponding metal bulks provided TM loading does not exceed 4 % of surface coverage. Analysis of the results show that La adatoms attach above the γ-graphyne acetylenic rings effectively *n*-doping the substrate and adopting an electron acceptor character, whereas this effect is less important for Ni adatoms, which attach in-plane the acetylenic ring. For Ni, charge density difference distribution plots show that the TM adopts an electron donor character, without strongly modifying the γ-graphyne band structure. The present results pave the ground for exploring other graphynes with tuneable acetylenic rings size to accommodate these and other SAs, with envisaged applications in heterogeneous catalysis, but also on nanotechnological processes of interest such as atomic filtering and electronic transport.

***Corresponding author. E-mail:** gamallo@ub.edu (Pablo Gamallo, ORCID: 0000-0002-8531-8063), jinylee@skku.edu (Jin Yong Lee)

Tables: 2 **Figures:** 3 **Proofs to:** Dr. Pablo Gamallo

Keywords: dispersion, single-atom catalyst, graphyne, heterogeneous catalysis.

Manuscript submitted to Theoretical Chemistry Accounts (February 16th, 2017)

1. Introduction

Supported single atoms (SAs) have driven considerable research attention in the last years, being the ultimate level of fine scattering. SAs are very appealing in heterogeneous catalysis, energy storage and nanotechnology.[1,2,3] Considering the later, special interest is focused on isolated atoms for data storage, *via* manipulation at will of spin states of a surface adatom, as observed for instance on silicon surfaces.[2, 4] These studies relied on manipulating the surface with a scanning tunnelling microscope (STM), a concomitant intricate process at the laboratory level. Nevertheless, a high level of success and reliability was obtained in the atomic manipulation of Ni or Co adatoms on graphene.[5] This is technically feasible, but only possible due to sensibly large energy barriers for diffusion of Co and Ni adatoms, which hinders sintering to small aggregates first, and nanoparticles later on, eventually losing their specific properties.

As far as heterogeneous catalysis is concerned, most of the commercial catalysts rely on using —scarce and expensive— active late transition metal elements finely dispersed on a high surface area support, typically an oxide. Supported metal nanoparticles are ubiquitous in heterogeneous catalysts,[6] since the increased surface/bulk atom ratio implies a large number of exposed active surface metal atoms. This nanoparticle dispersion considerably reduces the metal load for obtaining an equal catalytic activity, and so counteracts the cost of utilizing late transition metals. However, metal aggregates are typically irregularly formed in size and shape, thus opening a wide variety of possibilities in terms of activity and selectivity, with a concomitant loss of process control. The problems arising from the inhomogeneity of metal clusters has been tackled, for instance, with the so-called *soft landing* method, already applied for sintering small clusters of Pt landed on vanadia.[7] The homogeneity issue can be also solved by means of SA catalyst, thus reducing the catalyst size of the active phase to the ultimate level, and maximizing the catalyst power. Note that with SA catalysts every single atom could act *de facto* as an efficient catalyst.

Recently, synthesis of a Pt SA catalyst was successfully achieved using an iron oxide FeO_x support and taking advantage of surface defects as anchoring sites for Pt adatoms.[8] Along this line, isolated Pt atoms have been detected on CeO_2 nanoparticles by synchrotron radiation photoelectron spectroscopy and, with the help of density functional theory (DFT) calculations on nanoparticle models,[9] assigned to Pt^{2+} surface species located at stepped {001} surfaces. In this regard, the idea of exploiting defects to isolate metal adatoms has

become very appealing since, in some cases, the stability granted to a metal adatom through interaction with the support at these particular sites is stronger than the cohesive energy of the bulk metal itself. These strong adsorbate↔defect interactions have been observed for other systems of nanotechnological interest, such as the fullerene attachment to patterned vacancies on metal surfaces,[10] or even metal nanoparticle edge defects as templates for fullerene synthesis.[11] However, Pt/oxide systems, aside from notably modifying the electronic structure of the Pt adatom —positively charged due to a Pt→substrate charge transfer— rely on the existence of surface defects and the possibility of controlling their distribution. These defects are normally present in a low concentration, as well as in various forms, so that once again the problem of inhomogeneity emerges, but now from the substrate instead.

Another proposal to isolate metal adatoms is based on using organic molecular corrals on a defect-free surface. This methodology has been successfully applied to isolate Fe adatoms on a Cu(111) surface with a metal-organic surface framework with a honeycomb structure[12], although significant population of Fe dimers and trimers was also reported. Nevertheless, this achievement constitutes a paramount step in isolating metal adatoms on a metal surface, without a strong modification of the adatom electronic structure. A drawback of this otherwise appealing approach is that the surface area is determined by the Cu substrate. Inspired by this work, we decided to explore alternative materials featuring high surface area and, at the same time, ability to trap TM atoms in the same way as in the organic molecular corrals above mentioned.

A sensible choice would be graphene, a material widely considered as a support due to its excellent mechanical properties, being mostly chemically inert, as well as displaying a very large specific surface area of 2630 m^2 g^{-1}.[13] However, a recent DFT study predicts that TM adatoms on graphene will sinter in to large particles,[5] since the metal adatom↔graphene interaction is smaller than the metal bulk cohesive energy.[14] Thus, metal adatoms on graphene could only exist when adatom diffusion would be kinetically hindered at low temperatures, generally disrupting practical applications at ambient or high temperatures. In this sense, graphynes constitute an appealing alternative to graphene, and the present work explores this possibility in detail, finding that this is likely the case for La and Ni transition metals.

2. Computational Model and Methods

Graphynes are two-dimensional (2D) carbon allotropes formed from graphene by inserting acetylenic linkages into the honeycomb structure,[15] thus featuring C atoms with either sp^2 or sp hybridization. A plethora of graphynes can be envisaged, according to the planar arrangement and to the sp/sp^2 ratio. For instance α-, β- and γ-graphyne display $^3/_3$, $^2/_3$, and $^1/_3$ sp/sp^2 ratios, respectively.[16] Some of these graphynes have been found to display Dirac cones as in graphene, with similar or even better charge transport,[17] as recently confirmed experimentally *via* electrical measurements by STM means.[18] Note that, by introducing acetylenic linkages to graphene, the in-plane stiffness is reduced[16] with a concomitant benefit of increasing pore sizes, which in principle enables graphynes to be utilized as tuneable membrane separators.

Among the possible graphynes, γ-graphyne (Fig. 1) has been chosen here to study SA dispersion for three reasons: *i)* it is the one with highest structural stiffness, just half the value of graphene, and hence, still mechanically robust;[16] *ii)* it includes benzene type rings, similar to graphene, thus allowing for a convenient comparison while featuring at the same time the smallest possible acetylenic ring; and *iii)* new efficient synthetic routes already exist leading to γ-graphyne type patches.[19] The site selected for anchoring the TM atoms on the graphyne layer is the three-centre with the acetylenic ring (hereafter H1, see Fig. 1) that is the most stable adsorption site according to previous studies [3].

Indeed γ-graphyne is quite appealing for SA catalysts; it displays an specific surface area of 3440 $m^2\ g^{-1}$, even superior to graphene, and DFT calculations within the PBE functional predicted it to be a good substrate for SAs (Fe, Co, or Ni) based catalyst in the oxygen reduction reaction (ORR).[20] These metals were found to prefer adsorption in-plane in the acetylenic ring and with adsorption energies larger than the experimental metal bulk cohesive energy. However, a fair comparison requires referring to the cohesive energy as obtained at the same PBE level, since the method accuracy is disregarded otherwise. Recently, the potential of γ-graphyne as a substrate for Pt-group and coinage metal SA catalysts was investigated, reporting an out-of-plane adsorption above the acetylenic ring.[21] Atomic dispersion was claimed to occur because adatom adsorption strength was higher than metal dimer adsorption energy. However, one must point out that Pt bulk cohesive energy is substantially larger, and, with a proper diffusion, the system would be energetically driven to sinter.

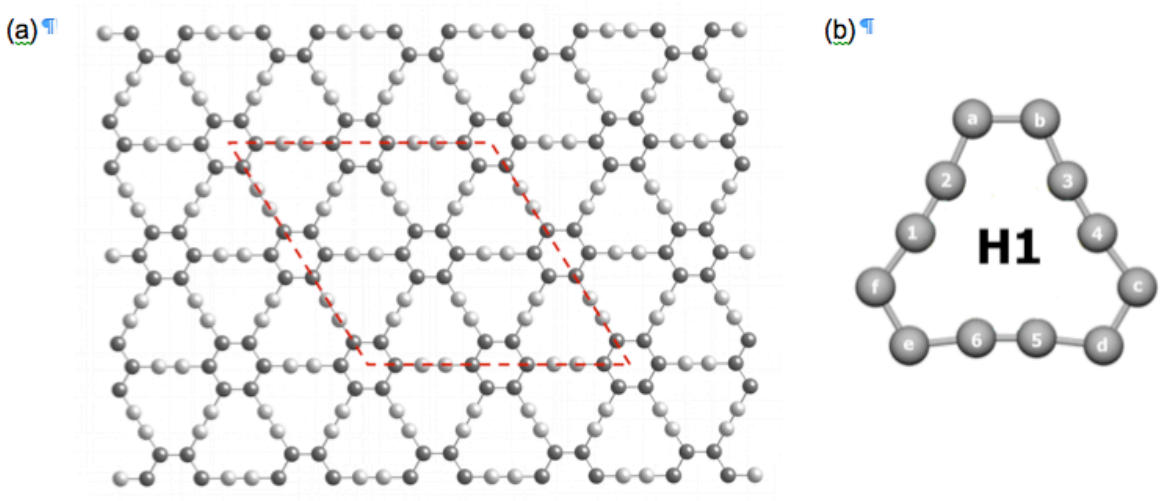

Figure 1. a) Pristine *p*(2×2) g-graphyne structure. Dark and light grey spheres denote sp^2 and *sp* C atoms, respectively. Dashed red lines delimit the employed supercell, b) Detail of biggest porous in γ-graphyne structure with the carbon atoms labelled for convenience (different labels identify carbon atoms hybridizations: numbers and letters stand for *sp* and sp^2 carbon atoms, respectively). This porous corresponds with the H1 site analysed throughout the study.

From the preceding discussion it is clear that a fair analysis of the metal adatom dispersion capability of γ-graphyne requires comparing calculated metal adsorption energies to calculated cohesive energies but with both quantities obtained at the same level of theory. Moreover, it is also interesting to include coverage effects, optimization of unit cell during adsorption as well as calculation of diffusion barriers, disregarded in the previous work.[20] Note also that since the cohesive energy of metallic nanoparticles slowly converges to that of the bulk, the present choice of using bulk cohesive energy values represents the most unfavourable scenario for SA. In fact, the use of finite nanoparticles cohesive energies as reference instead of bulk values would increase the number of metals with applications in SA catalysts.

Presently, we have investigated the structural, energetic, electronic, and magnetic properties of two TM atoms (Nickel and Lanthanum) interacting with γ-graphyne using periodic DFT calculations using the PBE implementation of the Generalized Gradient Approach (GGA) functionals. Briefly, electronic structure calculations have been carried out using the VASP code,[22] with core electrons described by Projector Augmented Wave

(PAW)[23] potentials. An optimized kinetic energy cut-off for the plane wave basis was set to 415 eV. The convergence threshold for the total energy was set to 10^{-5} eV and geometry optimizations were performed until forces applied on each atom were less than 0.01 eV $Å^{-1}$. A *p*(2×2) γ-graphyne supercell was used (Fig. 1), with a vacuum distance of at least 10 Å, sufficient to avoid interaction between periodically interleaved γ-graphyne sheets. An optimal Monkhorst-Pack **Γ**-centered 2×2×1 **k**-points grid was used for integration in the reciprocal space.[24] Optimized pristine γ-graphyne features a rhombohedral lattice with unit cell parameters of 6.880 Å (*i.e., a* = *b*), in very good agreement with previous calculations.[16,25]

The effect of adsorbed atoms in the cell relaxation was also considered although almost negligible deviations from the pristine cell parameters were observed, below 1 %. Contribution of dispersion terms has been introduced according to the D2 correction as proposed by Grimme.[26] The TM adsorption energy, E_{ads}, is calculated as the negative value of the energy difference between the TM adsorbed on the γ-graphyne and the sum of energies of pristine γ-graphyne and the isolated TM atom in its electronic ground state as computed at the spin polarized level, as previously reported.[14] Note that with the present definition, favourable adsorption implies positive adsorption energy value. TM bulk cohesive energies, E_{coh}, are taken from a previous study carried out at a comparable computational level.[14]

3. Results and discussion

3.1 Adsorption energies and structural properties

According to the DFT calculations two elements, Ni and La, present adsorption energies higher than the calculated cohesive energies (Table 1) at low coverages. According to this, for a $^{1}/_{48}$ coverage, defined as the $^{TM}/_{C}$ ratio (*i.e.,* ~2 % atomic coverage, hereafter at.), the adsorbed metal atoms would be energetically more stable and, hence, adsorption would drive towards SA fashion dispersion. Consequently, annealing would simply favour dispersion, opposite to common sintering. The main factor that favours such a big TM↔γ-graphyne interaction is the γ-graphyne metastability itself. The reduced C coordination, or, from the other side of the coin, the higher reactivity of *sp* C atoms implies an overall higher activity of γ-graphyne, and so, a stronger attachment of atoms and/or molecules onto. Figure 2 shows the adsorption of Ni and La atoms (2% at.) on γ-graphyne at the H1 site.

Table 1. PBE and PBE-D2 adsorption energies of Ni and La over γ-graphyne at different TM atomic concentration compared to cohesive energies as previously obtained at PBE level,[14] or here optimized at PBE-D2 level, and the reported experimental values.[27]

TM		**E_{ads} / eV**			**E_{coh} / eV**	
		2 % at.	**4 % at.**	**8 % at.**	**Theo.**	**Exp.**
Ni	**PBE**	5.33	5.45	4.18	4.87	4.44
	PBE-D2	5.49	5.60	4.46	5.34	
La	**PBE**	5.43	4.54	4.20	4.18	4.47
	PBE-D2	5.74	4.82	4.54	4.83	

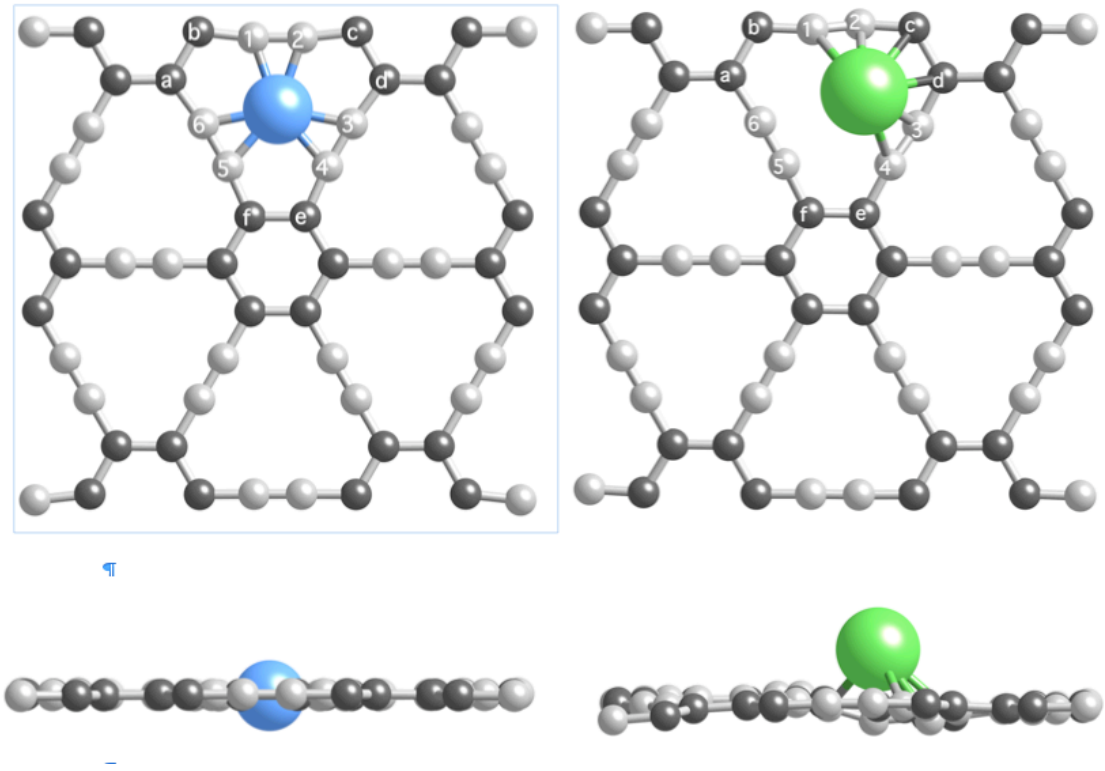

Figure 2. Adsorption of Ni (left) and La (right) atoms on γ-graphyne at 2% at. coverage. Top and bottom panels show top and side view, respectively. Dark and light grey spheres denote sp^2 and *sp* C atoms, respectively.

Adsorption energy for Ni and La over γ-graphyne at 2% at. coverage is 5.33 eV and 5.43 eV. The value for Ni is in agreement with the 5.18 eV reported in Ref. [3] obtained by means of LDA (Local Density Approximation) that usually drives to an underestimation of adsorption energies. In the case of La no previous results are available. Regarding TM load, 2 % at. coverage is energetically feasible for both Ni and La atoms by 0.46 (0.15) and 1.25 (0.91) eV, respectively, at PBE (PBE-D2) level. We have further considered the TM coverage by occupying half or all the acetylenic rings of the *p*(2×2) γ-graphyne supercell shown in Fig. 1, which correspond to 4 % and 8 % atomic loads, respectively. In the case of Ni dispersion the adsorption energy increases up to 4 % at. coverage since the Ni atoms are adsorbed in-plane with the γ-graphyne layer. In the case of La, as coverage increases the adsorption energies drop, in part due to the Pauli repulsion between La adatoms and, in part because of the reduced activity of γ-graphyne already stabilized by La adatoms (see below). In any case, a higher load of 4 % at. coverage is *a priori* energetically achievable for Ni by 0.58 (0.26) eV, whereas for La this is arguable, since at the PBE level is favourable by 0.36 eV, but becomes unfavourable by -0.01 eV when dispersion is taken into account. Dispersion effects do not seem to favour SA, yet the effect seems to stem out from bulk reference, where cohesive energies are greatly enhanced, by ~0.5-0.7 eV, whereas the increase is milder for adsorption energies, of about 0.2-0.3 eV.

In line with the previous, and deepening the structural analysis, Ni adatoms get trapped inside the acetylenic ring, and in-plane to γ-graphyne network, Fig. 2. This result is easy to understand from simple steric arguments. Among TMs in the periodic table, Ni features one of the smallest atomic radii. Moreover, in-plane adsorption allows for a better overlap between Ni *3d* and C *sp* orbitals, which is then translated into a stronger interaction. Moreover, a specific advantageous Ni↔γ-graphyne interaction involving Ni atomic orbitals and γ-graphyne bands is also responsible for Ni being atomically dispersed, at variance with other similar metals (*e.g.*, Co and Cu). It is worth pointing out that the Ni adsorption mode is markedly different from Group III TM La, which indeed presents one of the largest atomic radii and, consequently, would not fit into the acetylenic ring.

Consequently, La is adsorbed above the graphyne plane and displaced towards the benzene ring, in the acetylenic corner pocket, as shown in Fig. 2. Note that leftmost TMs in the periodic table are the most chemically active ones, and this fact, added to the above-mentioned higher activity of γ-graphyne explains the resulting strong interaction, yet the

particular La↔γ-graphyne overlap makes it different from other group III metals. The La adatoms are located 1.51 Å above the γ-graphyne mean plane with an almost negligible graphyne corrugation of 0.07 Å. Contribution of dispersion terms leads to insignificant structural changes (Table 2), a very similar electron density distribution, as well as a reduction of the adsorption energy evolution with coverage (~3–8 %). Hence, although contributing to the bonding, dispersion terms are responsible of a small percentage of the interaction only, with electronic interactions accounted for in the PBE exchange-correlation potential representing the largest contribution to the TM adatom adsorption on γ-graphyne.

The presence of the metal atoms on γ-graphyne structure produces distortion on nearest carbon atoms (Table 2). Ni atom gets adsorbed in H1 in-plane with γ-graphyne in a perfect symmetric conformation with TM-C(*sp*) and TM-C(sp^2) bonds distances equal to 1.952 Å and 2.864 Å, respectively (Figure 2, left). According to this, it is evident that the acetylenic carbon atoms are the responsible to give Ni such stable configuration, even lower than its own bulk. Moreover, in the γ-graphyne structure after Ni adsorption (2% at.) the *sp*-*sp* and *sp*-sp^2 bond distances become 4% and 1% longer than in pristine structure, respectively. Reversely, the sp^2-sp^2 bonds are slightly reduced (0.2%) when the Ni atom is present. These results agree with those reported in Ref. [3]. The higher volume of La atom makes impossible the adsorption in-plane and the metal atom remains adsorbed at a distance of 1.51 Å above the γ-graphyne surface and in a less symmetric fashion. In this case, the La atom prefers to adsorb close to a pair of acetylenic linkages at distances in the range 2.51-2.54 Å and to a pair of sp^2 C atoms at a distance 2.70 Å.

The adsorption of one Ni atom on γ-graphyne surface increases the C(*sp*)-C(*sp*) and C(*sp*)-C(sp^2) distances and diminishes the C(sp^2)-C(sp^2) ones with respect to the pristine surface by a factor of +3.92%, +0.92% and -0.21%, respectively. In this regard, the former bonds are weakened whereas the C(sp^2)-C(sp^2) bonds become stronger. In the case of La adsorption the situation is not so straightforward. Thus, those C-C bonds closer to the La adatom suffer the bigger changes. In the case of C(*sp*)-C(*sp*) bonds the distances are increased by +3.84% (1-2 and 3-4 C atoms) and +1.64% (5-6 C atoms). The C(*sp*)-C(sp^2) distances are reduced or increased depending on the distance to the La atom. The closest bonds to the La atom (2-c and 3-d) are reduced by -1.08% while the other bond distances are all increased +0.50% (1-b and 4-e) and +0.21% (6-a and 5-f). Finally, the C(sp^2)-C(sp^2)

distances increase in +3.65% (c-d), +0.28% (a-b) and +0.21% (e-f) with respect to the pristine γ-graphyne indicating that the closer the bond to the metal atom the higher perturbation to the bond.

Table 2. DFT C-C and TM-C bond distances for Ni and La atoms adsorbed on γ-graphyne for 2% at. coverage. The LDA distances reported in Ref. [3] are showed in square brackets. The bond distances for pristine γ-graphyne are also showed for comparison.

d (C – C)		**γ-graphyne**	**Ni + γ-graphyne 2% at.**	**La + γ-graphyne 2% at.**
sp-sp	1-2, 3-4, 5-6	1.223	1.271 [1.270]	1.270, 1.270, 1.243
sp-sp²	1-b, 2-c, 3-d, 4-e, 5-f, 6-a	1.408	1.421 [1.425]	1.415, 1.393, 1.393, 1.416, 1.411, 1.411
sp²-sp²	a-b, c-d, e-f	1.426	1.423 [1.415]	1.430, 1.478, 1.429
d (TM – C)				
TM – sp	TM-1, -2, -3, -4, -5, - 6		1.952	2.538, 2.510, 2.510, 2.539, 3.055, 3.054
TM –sp²	TM – a, -b, -c, -d, -e, -f		2.864, 2.865, 2.864, 2.864, 2.865, 2.865	3.721, 3.520, 2.695, 2.696, 3.523, 3.723

The effect of cell relaxation in the adsorption process has been also analysed. As shown in Table 3 the effect is quite small leading to γ-graphyne cells that retain the rhombohedral structure (*i.e., a = b*). In the case of Ni adsorption, the cell parameters are 6.898, 6.942, and 6.865 Å for 2, 4, and 8 % atomic coverages, respectively. The unit cell expands as the coverage increases up to 4 % whereas at 8 % a slight reduction in the unit cell is observed. This trend can be understood since up to 4 % at. coverages Ni adatoms prefer to be adsorbed in-plane γ-graphyne layer, resulting in an expansion of the unit cell. At higher coverages (*i.e.,* 8 %) Ni adatoms are shifted outward the surface and the γ-graphyne unit cell is again contracted. In the case of La, the γ-graphyne cell parameters increase slightly with coverage (Table 3). In the case of La adsorption, all the coverages explored present La atoms

dispersed over the γ-graphyne, and, hence, the expansion of the unit cell varies linearly with the concentration of adatoms, conversely to Ni atoms.

Table 3. Calculated PBE-D2 unit cell parameters in Å of Ni and La at different TM atomic concentration compared to pristine γ-graphyne unit cell ones.

Pristine γ-graphyne cell	**TM**	**2 % at.**	**4 % at.**	**8 % at.**
6.880	**Ni**	6.898	6.942	6.865
	La	6.880	6.887	6.900

Another aspect which is crucial to consider is the possible mobility of such dispersed Ni and La atoms, *i.e.* evaluating whether they would be anchored to the graphyne hollow, or, for instance, mobile yet avoiding the mutual recombination. Thus, atomic diffusion between most stable hollow sites has been evaluated by constrained relaxations fixing the planar position at diverse surface positions connecting vicinal hollow sites. Results reveal that La diffusion is favoured above the site bridging the benzene ring and an acetylenic link, with diffusion energy barriers of 0.52 and 0.51 eV as obtained at PBE and PBE-D2 levels, respectively. Consequently, La is likely to be mobile at moderate temperatures, *i.e.,* room temperature, and these results, together with the above commented preference for dispersion, suggest a complete spreading of La atoms when depositing small quantities of La over γ-graphyne. This picture differs for Ni, where Ni atoms are heavily anchored to the hollow sites, where the lowest possible diffusion energy barriers through the acetylenic ring are quite high: 3.08 and 3.19 eV at PBE and PBE-D2 levels, respectively. Thus, Ni could only diffuse over sites already occupied by other Ni atoms, with diffusion energy barriers around 0.2 eV as estimated at PBE level. These results point for a Ni immobilization where it lands, and, in case of Ni cluster landing, the dispersion of atoms in the immediate region.

3.2 Charge Transfer and band structures

The strong TM↔γ-graphyne interaction here reported apparently implies a TM→γ-graphyne charge transfer as well (*i.e.* effectively *n*-doping γ-graphyne) in line with previous results for the adsorption of these TM on graphene.[5] In fact, the charge transfer is large for La which, according to a Bader analysis of the electron density,[28] becomes rather oxidized with a net positive charge of +1.66 *e*. The charge transfer is smaller for Ni, with a value of +0.64 *e*, and so *n*-doping character cannot be claimed, see below. In addition, adsorption quenches the magnetic moment in both cases. We further analysed in Fig. 3 the electronic structure in terms of charge density difference (CDD) plots. The CDD isosurface for Ni, Fig. 3(a), shows how Ni adatom loses *d* electron density in the *xy* (graphyne) plane, and apparently three three-centre like bonds appear, each one linking the central Ni adatom with two *sp* C atoms of vicinal edges of the acetylenic ring. The acetylenic bonds appear to become slightly weakened, and some d_z^2 electron density of the central Ni atom becomes populated in a back-donation type interaction, which could have implications in a possible electron-donor catalytic activity, as the aforementioned ORR.[20] The out-of-plane bonding mode of La adatom disrupts the symmetry, Fig. 3(b). However, two three-centre bonds linking acetylenic and phenyl rings still remain, whereas two direct La↔C bonds with acetylenic C atoms are formed. Note that charge rearrangement suggests that La adatom also adopts an electron-donor role.

Further information can be extracted from the analysis of electronic band structure of SA on γ-graphyne, as well as that of pristine γ-graphyne. Thus, Fig. 4 shows the band energy eigenvalues along **Γ→K→M** directions. In accordance with previous studies, a direct band gap of 0.47 eV is found at **Γ** for pristine γ-graphyne.[16] The La adatoms, because of the rather sensible charge transfer above mentioned, effectively *n*-dope γ-graphyne, and so the conduction band becomes effectively populated, with a shift of the band gap centre down in energy by ~0.5 eV. Concerning Ni atoms, the smaller Bader charge does not imply an effective *n*-doping, and, actually, the γ-graphyne band gap remains unaltered. Indeed, this Bader charge implies a noticeable expansion and rearrangement of the Ni adatom electron density, which is less visible in the substrate. Nevertheless, the magnitude of the band gap is slightly affected, narrowing to values around 0.36 eV.

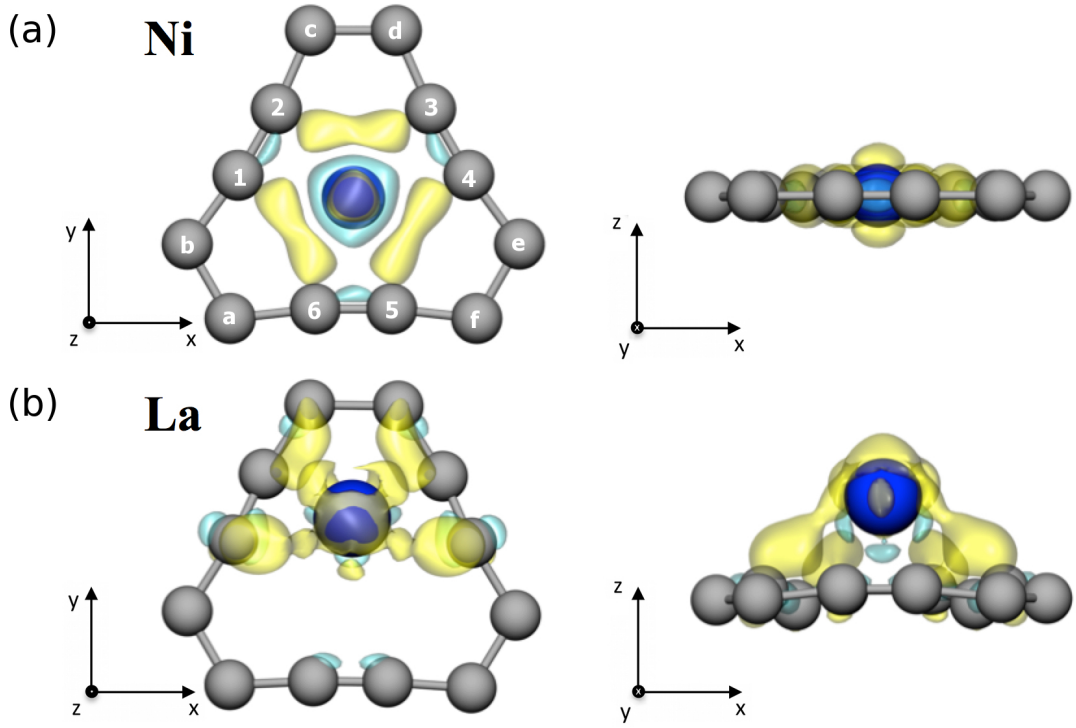

Fig. 3. Azimuthal (left) and side (right) views of most stable structures of Ni and La on the acetylenic ring of γ-graphyne and CDD plots of (a) Ni/γ-graphyne and (b) La/γ-graphyne. Electron accumulation and depletion isosurfaces 0.06 e $Å^{-3}$ are shown in yellow and light blue, respectively. Dark blue spheres denote TM atoms.

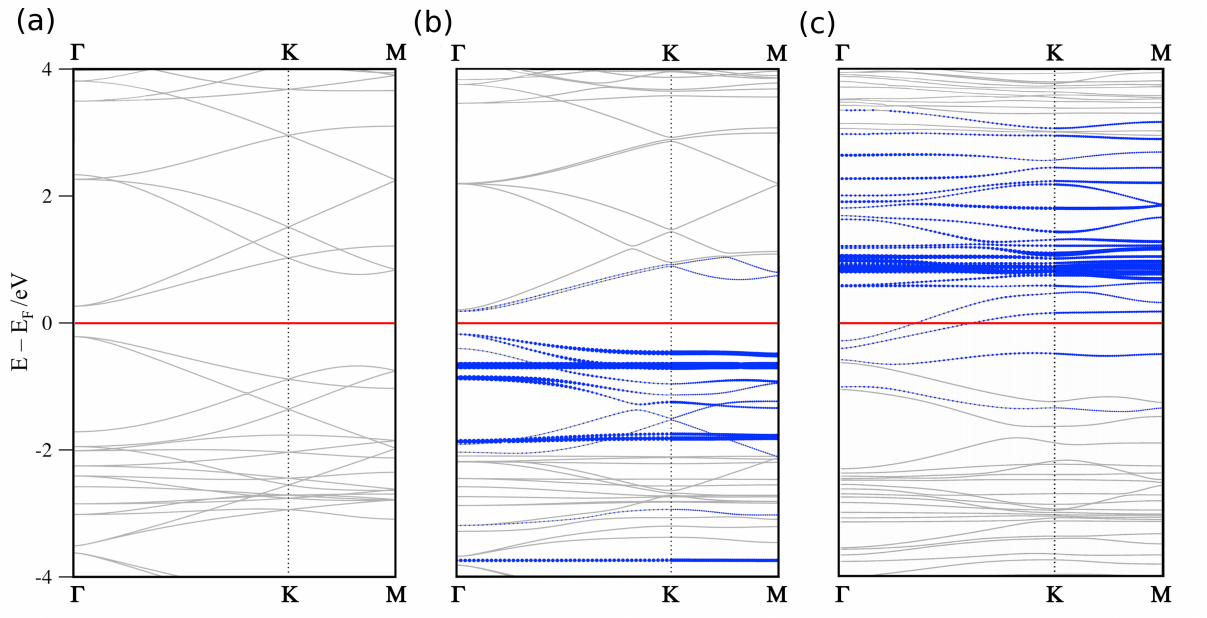

Fig. 4. Band structure of (a) pristine γ-graphyne, (b) Ni/γ-graphyne (2% at.), and (c) La/γ-graphyne (2% at.). Grey and blue lines denote γ-graphyne or TM associated bands, respectively. Red line denotes Fermi level energy, E_F.

4. Conclusions

In summary, we have shown that La and Ni atoms can be energetically driven to disperse in a SA fashion on γ-graphyne at low metal loading coverage. This is simply because, within the same computational scheme, calculated adsorption energies are larger than calculated bulk cohesive energies. It is worth pointing out again that this situation corresponds to the most possible unfavourable situation since the cohesive energies of finite nanoparticles are always lower than the bulk values. Results suggest that other group III (*e.g.,* Sc or Y) and 3d (*e.g.,* Co or Cu) TM atoms could also disperse in a SA fashion when comparing to nanoparticle average cohesive energies, and even to other TM atoms by tuning the acetylenic ring size using different types of graphynes and graphdyines.

For γ-graphyne both Ni and La adatoms feature three-centre bonds with the acetylenic ring. La atoms adsorb above the acetylenic ring and strongly *n*-dope γ-graphyne, while the oxidized nature of the La adatom confers an electron acceptor character. In the case of Ni, the adatoms occupy in-plane sites of the acetylenic ring, adopting a low electron donor character and reducing the γ-graphyne band gap to 0.36 eV.

In both cases, SA in γ-graphyne may result in systems of potential interest in catalysis. Our results indicate that γ-graphyne could catch interest as potential SA substrate in catalysis, but also in data storage, anchor points, or other aspects in nanotechnology area.

Acknowledgements

The work at SKKU was supported by the Korea government (Ministry of Science, ICT & Future Planning), the project EDISON grant (No. 2012M3C1A6035359) and the work at UB by Spanish *Ministerio de Economía y Competitividad* grants (CTQ2014-53987-R and CTQ2012-30751) and, in part, by *Generalitat de Catalunya* grants (2014SGR1582, 2014SGR97, and XRQTC). This project received funding from the European Union's Horizon 2020 research and innovation program under grant agreement no. 676580 with "The Novel Materials Discovery (NOMAD) Laboratory", a European Center of Excellence. P.G. thanks Generalitat de Catalunya for his Serra Húnter Associate Professorship. F.I. acknowledges additional support from the 2015 ICREA Academia Award for Excellence in University Research and F.V. thanks the Spanish *Ministerio de Economía y Competitividad*

for the *Ramón y Cajal* (RyC) postdoctoral grant (RYC-2012-10129).

References

[1] Yang XF, Wang A, Qiao B, Li J, Liu J, Zhang T (2013) Single-atom catalysts: a new frontier in heterogeneous catalysis. Acc Chem Res 46:1740-1748.

[2] Fuechsle M, Miwa JA, Mahapatra S, Ryu H, Lee S, Warschkow O, Hollenberg LCL, Klimeck G, Simmons MY (2012) A single-atom transistor. Nat Nanotechnol 7:242-246.

[3] Zhang L, Wu H (2016) Metal decorated graphyne and its boron nitride analog as versatile materials for energy storage: providing reference for the lithium-ion battery of wireless sensor nodes. Int. J. Hydrogen Energy 41:17471-17483.

[4] Pla JJ, Tan KY, Dehollain JP, Lim WH, Morton JJL, Jamieson DN, Dzurak AS, Morello A (2012) A singlet-atom electron spin qubit in silicon. Nature 489:541-545.

[5] Manadé M, Viñes F, Illas F (2015) Transition metal adatoms on graphene: a systematic density functional study, Carbon 95:525-534.

[6] Anderson JA, Fernández-García M (2011) Supported Metals in Catalysis; Catalytic Science Series. Imperial College Press, London.

[7] Vajda S, Pellin MJ, Greeley JP, Marshall CL, Curtiss LA, Ballentine GA, Elam JW, Catillon-Mucherie S, Redfern PC, Mehmood F, Zapol P (2009) Subnanometre platinum clusters as highly active and selective catalysts for the oxidative dehydrogenation of propane. Nat Mater 8:213-216.

[8] Qiao B, Wang A, Yang X, Allard LF, Jiang Z, Cui Y, Liu J, Zhang T (2011) Single-atom catalysis of CO oxidation using Pt_1/FeO_x. Nat Chem 3:634-641.

[9] Bruix A, Lykhach Y, Matoínová I, Neitzel A, Skála T, Tsud N, Vorokhta M, Stetsovych V, Sevcíková K, Myslivecek J, Fiala R, Václavu M, Prince KC, Bruyère S, Potin V, Illas F, Matolín V, Libuda J, Neyman KM (2014) Maximum noble-metal efficiency in catalytic materials: atomically dispersed surface platinum. Angew Chem Int Ed 53:10525-10530.

[10] Kaiser A, Viñes F, Illas F, Ritter M, Hagelberg F, Probst M (2014) Vacancy patterning and patterning vacancies: controlled self-assembly of fullerenes on metal surfaces. Nanoscale 6:10850-10858.

[11] Viñes F, Görling A (2011) Template-assisted formation of fullerenes from short-chain hydrocarbons by supported platinum nanoparticles. Angew Chem Int Ed 50:4611-4614.

[12] Pivetta M, Pacchioni GE, Schlickum U, Barth JV, Brune H (2015) Formation of Fe cluster superlattice in a metal-organic quantum-box network. Phys Rev Lett 110:086102.

[13] Bonaccorso F, Colombo L, Yu G, Stoller M, Tozzini V, Ferrari AC, Ruoff RS, Pellegrini V (2015) Graphene, related two-dimensional crystals, and hybrid systems for energy conversion

and storage. Science 347:1246501.

[14] Janthon P, Kozlov SM, Viñes F, Limtrakul J, Illas F (2013) Establishing the accuracy of broadly used density functionals in describing bulk properties of transition metals. J Chem Theory Comput 9:1631-1640.

[15] Baughman RH, Eckhardt H, Kertesz M (1987) Structure-property predictions for new planar forms of carbon: layered phases containing sp^2 and sp atoms, J Chem Phys 87:6687.

[16] Ruiz-Puigdollers A, Alonso G, Gamallo P (2016) First-principles study of structural, elastic and electronic properties of α-, β- and γ-graphyne. Carbon 96:879-887.

[17] Malko D, Neiss C, Viñes F, Görling A (2012) Competition for graphene: graphynes with direction-dependent Dirac cones. Phys Rev Lett 108:086804.

[18] Li Z, Smeu M, Rives A, Maraval V, Chauvin R, Ratner MA, Borguet E (2015) Towards graphyne molecular electronics. Nat Commun 6:6321.

[19] Bhaskar A, Guda R, Haley MM, Goodson III T (2006) Building symmetric two-dimensional two-photon materials. J Am Chem Soc 128:13972-13973.

[20] Srinivasu K, Ghosh SK (2013) Transition metal decorated graphyne: an efficient catalyst for oxygen reduction reaction. J Phys Chem C 117:26021-26028.

[21] Ma DW, Li T, Wang Q, Yang G, He C, Ma B, Lu Z (2015) Graphyne as a promising substrate for the noble-metal single-atom catalysts. Carbon 95:756-765.

[22] Kresse G, Furthmüller J (1996) Efficient iterative schemes for ab initio total-energy calculations using a plane-wave basis set. Phys Rev B 54:11169.

[23] Kresse G, Joubert D (1999) From ultrasoft pseudopotentials to the projector augmented-wave method. Phys Rev B 59:1758.

[24] Monkhorst HJ, Pack JD (1976) Special points for Brillouin-zone integrations. Phys Rev B 13:5188.

[25] Kang B, Liu H, Lee JY (2014) Oxygen adsorption on single layer graphyne: a DFT study. Phys Chem Chem Phys 16:974-980.

[26] Grimme S (2006) Semiempirical GGA-type density functional constructed with a long-range dispersion correction. J Comput Chem 27:1787-1799.

[27] Young DA (1991) Phase Diagrams of the Elements. University of California Press, Berkeley, USA.

[28] Bader RF (1990) Atoms in Molecules: a Quantum Theory. Oxford Science, Oxford, UK.